Antibunched Photons Emitted by a dc-Biased Josephson Junction

C. Rolland,[1,*] A. Peugeot,[1,*] S. Dambach,[2] M. Westig,[1] B. Kubala,[2] Y. Mukharsky,[1] C. Altimiras,[1] H. le Sueur,[1] P. Joyez,[1] D. Vion,[1] P. Roche,[1] D. Esteve,[1] J. Ankerhold,[2,†] and F. Portier[1,‡]
[1]DSM/IRAMIS/SPEC, CNRS UMR 3680, CEA, Université Paris-Saclay, 91190 Gif sur Yvette, France
[2]Institute for Complex Quantum Systems and IQST, University of Ulm, 89069 Ulm, Germany

(Received 17 October 2018; revised manuscript received 20 February 2019; published 10 May 2019)

We show experimentally that a dc biased Josephson junction in series with a high-enough-impedance microwave resonator emits antibunched photons. Our resonator is made of a simple microfabricated spiral coil that resonates at 4.4 GHz and reaches a 1.97 kΩ characteristic impedance. The second order correlation function of the power leaking out of the resonator drops down to 0.3 at zero delay, which demonstrates the antibunching of the photons emitted by the circuit at a rate of 6×10^7 photons per second. Results are found in quantitative agreement with our theoretical predictions. This simple scheme could offer an efficient and bright single-photon source in the microwave domain.

DOI: 10.1103/PhysRevLett.122.186804

Single-photon sources constitute a fundamental resource for many quantum information technologies, notably secure quantum state transfer using flying photons. In the microwave domain, although photon propagation is more prone to losses and thermal photons present except at extremely low temperature, applications can nevertheless be considered [1,2]. Single microwave photons were first demonstrated in Ref. [3] using the standard design of single-photon emitters: an anharmonic atomlike quantum system excited from its ground state relaxes by emitting a single photon on a well-defined transition before it can be excited again. The first and second order correlation functions of such a source [4] demonstrate a rather low photon flux limited by the excitation cycle duration, but an excellent antibunching of the emitted photons. We follow a different approach, where the tunneling of discrete charge carriers through a quantum coherent conductor creates photons in its embedding circuit. The resulting quantum electrodynamics of this type of circuits [5–11] has been shown to provide, e.g., masers [12–15], simple sources of nonclassical radiation [16–18], or near quantum-limited amplifiers [19]. When the quantum conductor is a Josephson junction, dc biased at voltage V in series with a linear microwave resonator, exactly one photon is created in the resonator each time a Cooper pair tunnels through the junction, provided that the Josephson frequency $2eV/h$ matches the resonator's frequency [20]. We demonstrate here that in the strong coupling regime between the junction and the resonator, the presence of a single photon in the resonator inhibits the further tunneling of Cooper pairs, leading to the antibunching of the photons leaking out of the resonator [21,22]. Complete antibunching is expected when the characteristic impedance of the resonator reaches $Z_c = 2R_Q/\pi$, with $R_Q = h/(2e)^2 \simeq 6.45$ kΩ the superconducting resistance quantum. This regime, for which the analogue of the fine structure constant of the problem is of order 1, has recently attracted attention [23,24], as it allows the investigation of many-body physics with photons [25,26] or ultrastrong coupling physics [27], offering new strategies for the generation of nonclassical radiation [28].

The simple circuit used in this work is represented in Fig. 1(a): a Josephson junction is coupled to a microwave resonator of frequency ν_R and characteristic impedance Z_c, and biased at a voltage V smaller than the gap voltage $V_{\rm gap} = 2\Delta/e$, where $-e$ is the electron charge and Δ the superconducting gap, so that single electron tunneling is impossible. The time-dependent Hamiltonian

$$H = (a^\dagger a + 1/2)h\nu_R - E_J \cos[\phi(t)] \qquad (1)$$

of the circuit is the sum of the resonator and Josephson Hamiltonians. Here a is the photon annihilation operator in the resonator, E_J is the Josephson energy of the junction, $\phi(t) = 2eVt/\hbar - \sqrt{r}(a + a^\dagger)$ is the phase difference across the junction (conjugate to the number of Cooper pairs transferred across the junction), and $r = \pi Z_c/R_Q$ is the charge-radiation coupling in this one-mode circuit [29]. The nonlinear Josephson Hamiltonian thus couples Cooper pair transfer to photon creation in the resonator. This results in inelastic Cooper pair tunneling: a dc current flows in this circuit when the electrostatic energy provided by the voltage source upon the transfer of a Cooper pair corresponds to the energy of an integer number k of photons created in the resonator: $2eV = kh\nu_R$. The steady state occupation number $\bar{n}$ in the resonator results from the balance between the Cooper pair tunneling rate and the leakage rate to the measurement line. For $k = 1$—the

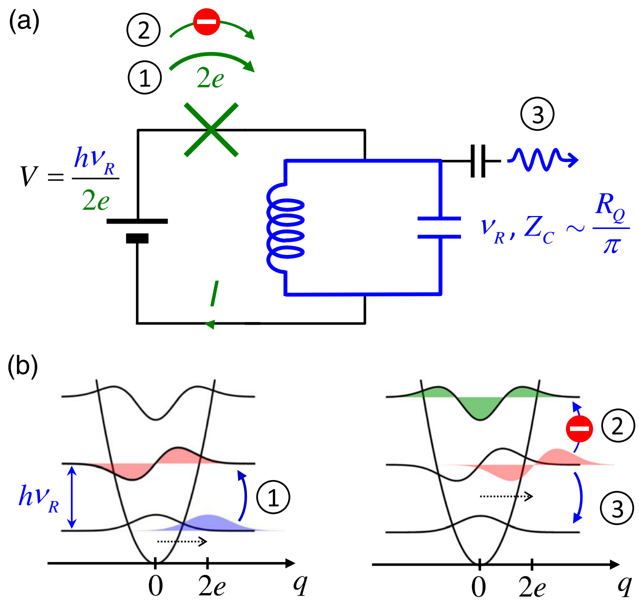

FIG. 1. Principle of the experiment: (a) A Josephson junction in series with a resonator of frequency ν_R and characteristic impedance Z_c of the order of $R_Q = h/(2e)^2$ is voltage biased so that each Cooper pair that tunnels produces a photon in the resonator (1). (b) Photon creation and relaxation: A tunneling Cooper pair shifts the charge on the resonator capacitance by $2e$. The tunneling rate $\Gamma_{n\to n+1}$ starting with the resonator in Fock state $|n\rangle$ is proportional to the overlap between the wave function $\Psi_n(q)$ shifted by $2e$ and $\Psi_{n+1}(q)$. This overlap depends itself on Z_C via the curvature of the resonator energy. At a critical Z_c, $\Gamma_{1\to 2} = 0$ and no additional photons can be created (2) until the photon already present has leaked out (3). The photons produced are thus antibunched, which is revealed by measuring the $g^{(2)}$ function of the leaked radiation.

resonance condition of the ac Josephson effect—each Cooper pair transfer creates a single photon. The theory of dynamical Coulomb blockade (DCB) [29–31] predicts that, in the limit of small coupling r, the power emitted into an empty resonator,

$$\mathcal{P} = \frac{2e^2 E_J^{*2}}{\hbar^2} \mathrm{Re}\, Z(\nu = 2eV/h), \tag{2}$$

coincides with the ac Josephson expression, albeit with a reduced effective Josephson energy $E_J^* = E_J e^{-r/2}$ renormalized by the zero-point phase fluctuations of the resonator [21–23,32,49–51]. In the strong-coupling regime ($r \simeq 1$), however, the single rate description above breaks down as a single photon in the resonator already influences further emission processes, as explained in Fig. 1(b).

A more sophisticated theory [21,22] addressing this regime considers the Hamiltonian (1) in the rotating-wave approximation at the resonance condition $2eV = h\nu_R$ for single-photon creation. Expressed in the resonator Fock state basis $\{|n\rangle\}$, H reduces to $H^{\mathrm{RWA}} = -(E_J/2)\sum_n (h^{\mathrm{RWA}}_{n,n+1}|n\rangle\langle n+1| + \mathrm{H.c.})$, with the transition matrix elements

$$h^{\mathrm{RWA}}_{n,n+1} = \langle n|\exp[i\sqrt{r}(a^\dagger + a)]|n+1\rangle. \tag{3}$$

Describing radiative losses via a Lindblad superoperator, one gets the second order correlation function for vanishing occupation number $\bar{n} \ll 1$ [21,22]:

$$g^{(2)}(\tau) = \frac{\langle a^\dagger(0)a^\dagger(\tau)a(\tau)a(0)\rangle}{\langle a^\dagger a\rangle^2} = \left(1 - \frac{r}{2}\exp(-\kappa\tau/2)\right)^2, \tag{4}$$

with κ the photon leakage rate of the resonator. In the low coupling limit $r \ll 1$, where $h^{\mathrm{RWA}}_{n,n+1}$ scales as $\sqrt{n+1}$, one recovers the familiar Poissonian correlations $g^{(2)}(0) = 1$. On the contrary, at $r = 2$ ($Z_c = 4.1$ kΩ), $h^{\mathrm{RWA}}_{1,2} = 0$ and Eq. (4) yields perfect antibunching of the emitted photons: $g^{(2)}(0) = 0$. In this regime, as illustrated by Fig. 1, a first tunnel event bringing the resonator from Fock state $|0\rangle$ to $|1\rangle$ cannot be followed by a second one as long as the photon has not been emitted in the line. This is the mechanism involved in the Frank-Condon effect and relies on the reduction of the matrix element of the Josephson Hamiltonian between the one and two photon states of the cavity as the coupling parameter r increases from 0 to 2, where it vanishes. It is thus different from the mechanism at work in the recent work of Grimm and co-workers [52], which relies on the charge relaxation induced by a large on-chip resistance.

Standard on-chip microwave resonator designs yield characteristic impedances of the order of 100 Ω, i.e., $r \sim 0.05$. To approach $r \sim 1$–2, we have microfabricated a resonator with a spiral inductor etched in a 150 nm niobium film sputtered onto a quartz substrate, chosen for its low dielectric constant ($\epsilon_r \simeq 3.8$), which was then connected to a SQUID loop, of normal resistance $R_t = 222 \pm 3$ kΩ, acting as a flux-tunable Josephson junction (see Fig. 2). The outgoing radiation was collected in a 50 Ω line through an impedance-matching stage aiming at lowering the resonator quality factor. The geometry of the resonator was optimized using the microwave solver Sonnet, predicting a resonant frequency $\nu_R = 5.1$ GHz, with a characteristic impedance of 2.05 kΩ, corresponding to $r = 1.0$, and a quality factor $Q = 2\pi\nu_r/\kappa = 42$ [32]. The actual values measured using the calibration detailed in the Supplemental Material [32] are $\nu_r = 4.4$ GHz, $Q = 36.6$, and a characteristic impedance $Z_c = 1.97 \pm 0.06$ kΩ, corresponding to a coupling parameter $r = 0.96 \pm 0.03$, and thus to an expected $E_J^*/E_J = 0.62 \pm 0.01$. We attribute the small difference between design and experimental values to a possible underestimation in our microwave simulations of the capacitive coupling of the resonator to the surrounding grounding box.

The sample is placed in a shielded sample holder thermally anchored to the mixing chamber of a dilution

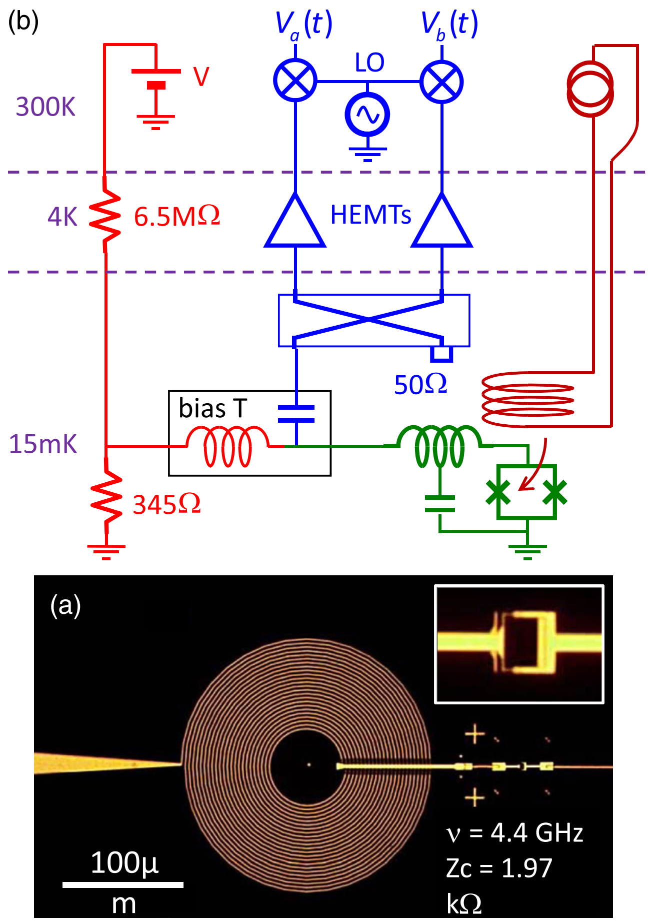

FIG. 2. Experimental setup. (a) Optical micrography of the sample showing the Al/AlOx/Al SQUID (inset) implementing the Josephson junction and the resonator made of a Nb spiral inductor with stray capacitance to ground. (b) Schematic of the circuit showing the sample (green), the coil circuit for tuning the Josephson energy (brown), the dc bias line (red), and the bias tee connected to the microwave line (blue) with bandpass filters, isolators (not shown here), and a symmetric splitter connected to two measurement lines with amplifiers at 4.2 K and demodulators at room temperature [32].

refrigerator at $T = 12$ mK. As shown in Fig. 2, the sample is connected to a bias tee, with a dc port connected to a filtered voltage divider, and an rf port connected to a 90° hybrid coupler acting as a microwave beam splitter towards two amplified lines with an effective noise temperature of 13.8 K. After bandpass filtering at room temperature, the signals in these two channels $V_a(t)$, $V_b(t)$ are down converted to the 0–625 MHz frequency range using two mixers sharing the same local oscillator at $\nu_{\rm LO} = 4.71$ GHz, above the resonator frequency. The output signals are then digitized at 1.25 GSamples/s to measure their two quadratures, and the relevant correlation functions are computed numerically.

In Fig. 3(a), the measured 2D emission map as a function of bias voltage and frequency shows the single-photon regime along the diagonal. A cut at the resonator frequency

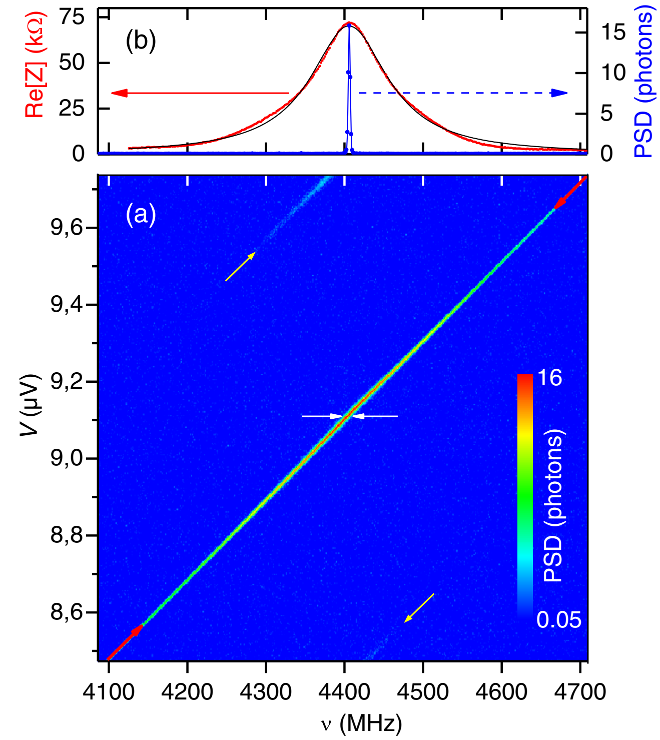

FIG. 3. Emitted microwave power and impedance seen by the junction. (a) 2D map of the emitted power spectral density (PSD) as a function of the frequency ν and bias voltage V, expressed in photon occupation number (logarithmic color scale). (b) Spectral line at $V = 9.11$ μV (blue points) obtained from a cut in the 2D map along the horizontal white arrows and real part of the impedance $\mathrm{Re}[Z(\nu)]$ seen by the SQUID (red points). The solid blue (black) line is a Gaussian (Lorentzian) fit.

[blue line in Fig. 3(b)] reveals an emission width of 2.9 MHz, which we attribute to low frequency fluctuations of the bias voltage, mostly of thermal origin. Two faint lines (pointed by the oblique yellow arrows) also appear at $2eV = h(\nu \pm \nu_P)$, and correspond to the simultaneous emission of a photon in the resonator and the emission or absorption of a photon in a parasitic resonance of the detection line at $\nu_P = 325$ MHz. Comparing the weight of these peaks to the main peak at $2eV = h\nu$ yields a 61 Ω characteristic impedance of the parasitic mode and a 15 mK mode temperature in good agreement with the refrigerator temperature.

We now set the bias at $V = h\nu_r/2e = 9.1$ μV, and we detect the output signals of the two amplifiers in a frequency band of 525 MHz (~4.4 resonator's FWHM) centered at the emission frequency ν_R. This apparently large detection window—180 times wider than the emission line, see Fig. 3(b)—is actually barely enough to measure the fast fluctuations occurring at frequencies up to the inverse resonator lifetime. An even larger bandwidth would bring the measured $g^{(2)}$ closer to the expected value of Eq. (4) but would also increase the parasitic fluctuations due to the amplifiers' noise and increase the necessary averaging time. Our choice is thus a compromise, leading to a 15-day long averaging for the lowest occupation number. From the down-converted signals, we rebuild their complex envelopes $S_{a,b}(t)$ [32,53]. We now use two alternative methods to extract $g^{(2)}(\tau)$. First, we obtain the instantaneous powers $P_{a,b}(t) = |S_{a,b}(t)|^2$, and extract

$$g^{(2)}(\tau) = \frac{\langle P_a(t)P_b(t+\tau)\rangle}{\langle P_a(t)\rangle\langle P_b(t+\tau)\rangle} \quad (5)$$

from their cross-correlations. Here, the sample's weak contribution has to be extracted from the large background noise of the amplifiers, which we measure by setting the bias voltage to zero. To overcome this complication and get a better precision on $g^{(2)}$, we compute the complex cross-signal $C(t) = S_a{}^*(t)S_b(t)$, which is proportional to the power emitted by the resonator and has a negligible background average contribution. $g^{(2)}(\tau)$ can then be extracted from the correlation function of $C(t)$ and $C^*(t)$ [32]. As $g^{(2)}(\tau)$ is real and the instantaneous noise on $C(t)$ is spread evenly between real and imaginary parts, this also improves the signal to noise ratio by $\sqrt{2}$.

Both methods gave the same results within their standard deviations, and the $g^{(2)}$ values shown in Fig. 4 correspond to the average of the two procedures. As we decrease the photon emission rate by adjusting E_J with the magnetic flux threading the SQUID, $g^{(2)}(0)$ decreases. For the lowest measured emission rate of 60 millions photons per second, corresponding to an average resonator population of 0.08 photons, $g^{(2)}(0)$ goes down to 0.31 ± 0.04, in good agreement with the theoretical prediction of 0.27, cf. Eq. (4) for $r = 0.96$. This is the main result of this work, which demonstrates a significant antibunching of the emitted photons. In agreement with Eq. (4), the characteristic timescale of the $g_2(\tau)$ variations coincides with the 1.33 ns resonator lifetime deduced from the calibrations. As our design did not reach $r = 2$, the transition from $|1\rangle$ to $|2\rangle$ is not completely forbidden, and from then on, transitions from $|2\rangle$ to $|3\rangle$ and higher Fock states can occur. The larger E_J, the more likely to have 2 photons and hence photon bunching. To predict the time-dependent $g^{(2)}(\tau)$ for arbitrary E_J, we solve the full quantum master equation

$$\dot{\rho} = -\frac{i}{\hbar}[H^{\mathrm{RWA}}, \rho] + \frac{\kappa}{2}(2a\rho a^\dagger - a^\dagger a\rho - \rho a^\dagger a). \quad (6)$$

This approach also allows for the quantitative modeling of the experimental measurement via a four-time correlator [32]. Properly accounting for filtering in the measurement chain (see Refs. [4,53] and Supplemental Material [32]), this description accurately reproduces the experimental results in Fig. 4 (lines) without any fitting parameters.

We finally probe the renormalization of E_J by the zero point fluctuations of the resonator using Eq. (2). This requires us to maintain the resonator photon population much below 1, which should be obtained by reducing the Josephson energy using the flux through the SQUID. However, magnetic hysteresis due to vortex pinning in the nearby superconducting electrodes prevented us from ascribing a precise flux to a given applied magnetic field, the only straightforward and reliable working point at our disposal thus occurring at zero magnetic flux and maximum Josephson energy. To ensure that the SQUID remains in the DCB regime even at this maximum E_J, and ensure a

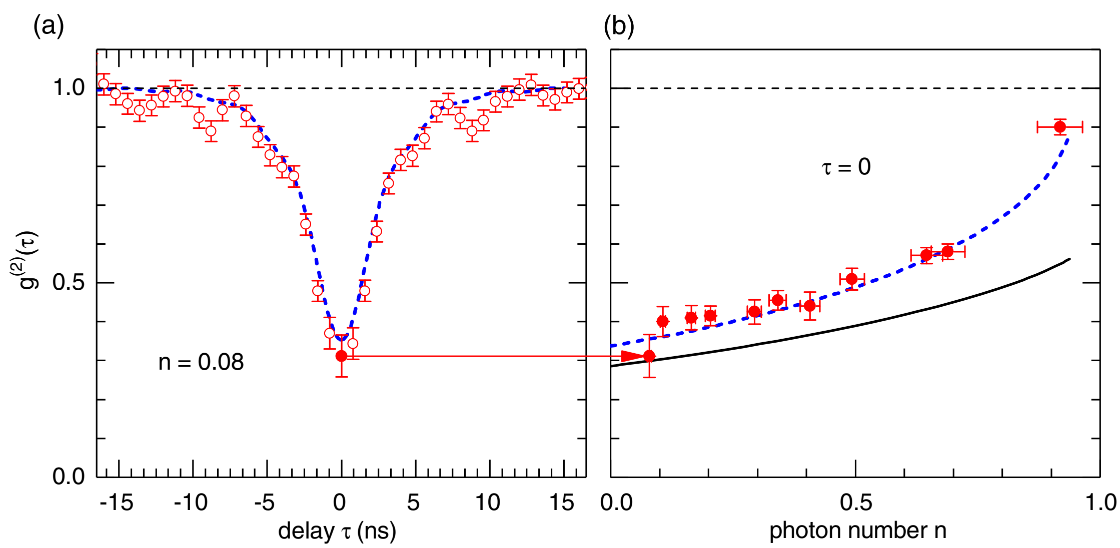

FIG. 4. Antibunching of the emitted radiation at bias $V = h\nu_R/2e = 9.11\ \mu\mathrm{V}$. (a) Experimental (dots) and theoretical (dashed line) second order correlation function $g^{(2)}$ as a function of delay τ for $n = 0.08$ photons in the resonator. Error bars indicate $\pm$ the statistical standard deviation. (b) Experimental (dots) and theoretical (dashed line) $g^{(2)}(0)$ as a function of n. The solid line is the theoretical prediction not taking into account the finite detection bandwidth.

low enough photon population, we select a bias voltage $V = 10.15\ \mu\text{V}$ yielding radiation at 4.91 GHz, far off the resonator frequency. Here again, the normal current shot noise is used as a calibrated noise source to measure *in situ* $G\text{Re}\,Z(\nu = 4.91\ \text{GHz})$. The effective Josephson energy $E_J^* = 1.86 \pm 0.02\ \mu\text{eV}$ extracted in this way is significantly smaller than the Ambegaokar-Baratoff value of $E_J = 3.1 \pm 0.03\ \mu\text{eV}$, and in good agreement with our prediction of $E_J^* = 1.84 \pm 0.03\ \mu\text{eV}$ [54], taking also into account the phase fluctuations coming from the parasitic mode at ν_p and its harmonics.

In conclusion, we have explored a new regime of the quantum electrodynamics of coherent conductors by strongly coupling a dc biased Josephson junction to its electromagnetic environment, a high-impedance microwave resonator. This enhanced coupling first results in a sizable renormalization of the effective Josephson energy of the junction. Second, it provides an extremely simple and bright source of antibunched photons. Appropriate time shaping either of the bias voltage [55], or the resonator frequency, or the Josephson energy [52] should allow for on-demand single-photon emission. This new regime that couples quantum electrical transport to quantum electromagnetic radiation opens the way to new devices for quantum microwave generation. It also allows many fundamental experiments like investigating high photon number processes, parametric transitions in the strong coupling regime [21,22,56,57], the stabilization of a Fock state by dissipation engineering [55], or the development of a new type of Qbit based on the Lamb shift induced by the junction [58].

We thank B. Huard, S. Seidelin, and M. Hofheinz for useful discussions. This work received funding from the European Research Council under the European Unions Programme for Research and Innovation (Horizon 2020)/ERC Grant Agreement No. 639039. We gratefully acknowledge partial support from LabEx PALM (ANR-10-LABX-0039-PALM), ANR Contracts ANPhoTeQ and GEARED, from the ANR-DFG Grant JosePhSCharLi, and from the ERC through the NSECPROBE grant, from IQST and the German Science Foundation (DFG) through AN336/11-1. S. D. acknowledges financial support from the Carl-Zeiss-Stiftung.

[*]These authors contributed equally to this work.
[†]joachim.ankerhold@uni-ulm.de
[‡]fabien.portier@cea.fr

[1] Z.-L. Xiang, M. Zhang, L. Jiang, and P. Rabl, Phys. Rev. X **7**, 011035 (2017).
[2] X. Gu, A. F. Kockum, A. Miranowicz, Y.-X. Liu, and F. Nori, Phys. Rep. **718–719**, 1 (2017).
[3] A. A. Houck *et al.*, Nature (London) **449**, 328 (2007).
[4] D. Bozyigit *et al.*, Nat. Phys. **7**, 154 (2011).
[5] A. Cottet, T. Kontos, and B. Douçot, Phys. Rev. B **91**, 205417 (2015).
[6] O. Dmytruk, M. Trif, C. Mora, and P. Simon, Phys. Rev. B **93**, 075425 (2016).
[7] C. Mora, C. Altimiras, P. Joyez, and F. Portier, Phys. Rev. B **95**, 125311 (2017).
[8] C. Altimiras, F. Portier, and P. Joyez, Phys. Rev. X **6**, 031002 (2016).
[9] A. L. Grimsmo, F. Qassemi, B. Reulet, and A. Blais, Phys. Rev. Lett. **116**, 043602 (2016).
[10] J. Leppäkangas, G. Johansson, M. Marthaler, and M. Fogelström, New J. Phys. **16**, 015015 (2014).
[11] J. Leppäkangas, G. Johansson, M. Marthaler, and M. Fogelström, Phys. Rev. Lett. **110**, 267004 (2013).
[12] Y.-Y. Liu, K. D. Petersson, J. Stehlik, J. M. Taylor, and J. R. Petta, Phys. Rev. Lett. **113**, 036801 (2014).
[13] J.-C. Forgues, C. Lupien, and B. Reulet, Phys. Rev. Lett. **114**, 130403 (2015).
[14] F. Chen, J. Li, A. D. Armour, E. Brahimi, J. Stettenheim, A. J. Sirois, R. W. Simmonds, M. P. Blencowe, and A. J. Rimberg, Phys. Rev. B **90**, 020506(R) (2014).
[15] M. C. Cassidy, A. Bruno, S. Rubbert, M. Irfan, J. Kammhuber, R. N. Schouten, A. R. Akhmerov, and L. P. Kouwenhoven, Science **355**, 939 (2017).
[16] J.-C. Forgues, C. Lupien, and B. Reulet, Phys. Rev. Lett. **113**, 043602 (2014).
[17] M. J. Gullans, J. Stehlik, Y.-Y. Liu, C. Eichler, J. R. Petta, and J. M. Taylor, Phys. Rev. Lett. **117**, 056801 (2016).
[18] M. Westig *et al.*, Phys. Rev. Lett. **119**, 137001 (2017).
[19] S. Jebari, F. Blanchet, A. Grimm, D. Hazra, R. Albert, P. Joyez, D. Vion, D. Esteve, F. Portier, and M. Hofheinz, Nat. Electron. **1**, 223 (2018).
[20] M. Hofheinz, F. Portier, Q. Baudouin, P. Joyez, D. Vion, P. Bertet, P. Roche, and D. Esteve, Phys. Rev. Lett. **106**, 217005 (2011).
[21] V. Gramich, B. Kubala, S. Rohrer, and J. Ankerhold, Phys. Rev. Lett. **111**, 247002 (2013).
[22] S. Dambach, B. Kubala, V. Gramich, and J. Ankerhold, Phys. Rev. B **92**, 054508 (2015).
[23] J. Puertas Martínes *et al.*, npj Quantum Inf. **5**, 19 (2019).
[24] R. Kuzmin, R. Mencia, N. Grabon, N. Mehta, Y.-H. Lin, and V. E. Manucharyan, arXiv:1805.07379.
[25] K. Le Hur, Phys. Rev. B **85**, 140506(R) (2012).
[26] M. Goldstein, M. H. Devoret, M. Houzet, and L. I. Glazman, Phys. Rev. Lett. **110**, 017002 (2013).
[27] B. Peropadre, D. Zueco, D. Porras, and J. J. García-Ripoll, Phys. Rev. Lett. **111**, 243602 (2013).
[28] N. Gheeraert, S. Bera, and S. Florens, New J. Phys. **19**, 023036 (2017).
[29] G.-L. Ingold and Y. V. Nazarov, in *Single Charge Tunneling*, edited by H. Grabert and M. H. Devoret (Plenum, New York, 1992).
[30] D. Averin, Y. Nazarov, and A. Odintsov, Physica (Amsterdam) **(165–166)B**, 945 (1990).
[31] T. Holst, D. Esteve, C. Urbina, and M. H. Devoret, Phys. Rev. Lett. **73**, 3455 (1994).
[32] See Supplemental Material at http://link.aps.org/supplemental/10.1103/PhysRevLett.122.186804 for more details about the fabrication process and measurement procedure, which includes Refs. [33–48].

[33] G.-L. Ingold and H. Grabert, Europhys. Lett. **14**, 371 (1991).

[34] B. Kubala, V. Gramich, and J. Ankerhold, Phys. Scr. **T165**, 014029 (2015).

[35] A. D. Armour, B. Kubala, and J. Ankerhold, Phys. Rev. B **96**, 214509 (2017).

[36] D. Walls and G. Milburn, *Quantum Optics* (Springer, Berlin, Heidelberg, 2009), ISBN 9783540814887.

[37] S. Boutin, D. M. Toyli, A. V. Venkatramani, A. W. Eddins, I. Siddiqi, and A. Blais, Phys. Rev. Applied **8**, 054030 (2017).

[38] E. del Valle, A. Gonzalez-Tudela, F. P. Laussy, C. Tejedor, and M. J. Hartmann, Phys. Rev. Lett. **109**, 183601 (2012).

[39] E. del Valle, New J. Phys. **15**, 025019 (2013).

[40] C. Dory, K. A. Fischer, K. Müller, K. G. Lagoudakis, T. Sarmiento, A. Rundquist, J. L. Zhang, Y. Kelaita, N. V. Sapra, and J. Vučković, Phys. Rev. A **95**, 023804 (2017).

[41] C. M. Caves, Phys. Rev. D **26**, 1817 (1982).

[42] J. M. Fink, M. Kalaee, A. Pitanti, R. Norte, L. Heinzle, M. Davanço, K. Srinivasan, and O. Painter, Nat. Commun. **7**, 12396 (2016).

[43] M.-C. Harabula, T. Hasler, G. Fülöp, M. Jung, V. Ranjan, and C. Schönenberger, Phys. Rev. Applied **8**, 054006 (2017).

[44] T. Hasler, M. Jung, V. Ranjan, G. Puebla-Hellmann, A. Wallraff, and C. Schönenberger, Phys. Rev. Applied **4**, 054002 (2015).

[45] C. Altimiras, O. Parlavecchio, P. Joyez, D. Vion, P. Roche, D. Esteve, and F. Portier, Appl. Phys. Lett. **103**, 212601 (2013).

[46] T. Holmqvist, M. Meschke, and J. P. Pekola, J. Vac. Sci. Technol. B **26**, 28 (2008).

[47] I. Wolff, *Coplanar Microwave Integrated Circuits* (Wiley, Hoboken/New Jersey, 2006).

[48] G. J. Dolan, Appl. Phys. Lett. **31**, 337 (1977).

[49] G. Schön and A. Zaikin, Phys. Rep. **198**, 237 (1990).

[50] H. Grabert, G.-L. Ingold, and B. Paul, Europhys. Lett. **44**, 360 (1998).

[51] P. Joyez, Phys. Rev. Lett. **110**, 217003 (2013).

[52] A. Grimm *et al.*, Phys. Rev. X **9**, 021016 (2019).

[53] M. P. da Silva, D. Bozyigit, A. Wallraff, and A. Blais, Phys. Rev. A **82**, 043804 (2010).

[54] The flux jumps due to vortex depinning were slow enough that we could compensate for them manually. We could thus obtain the total flux dependance of the emitted power, whose fit with a sinusoidal law yields the same value for E_J within experimental errors and a negligible asymmetry.

[55] J.-R. Souquet and A. A. Clerk, Phys. Rev. A **93**, 060301(R) (2016).

[56] C. Padurariu, F. Hassler, and Y. V. Nazarov, Phys. Rev. B **86**, 054514 (2012).

[57] S. Meister, M. Mecklenburg, V. Gramich, J. T. Stockburger, J. Ankerhold, and B. Kubala, Phys. Rev. B **92**, 174532 (2015).

[58] J. Estève, M. Aprili, and J. Gabelli, arXiv:1807.02364.